Eur. Phys. J. Spec. Top.
https://doi.org/10.1140/epjs/s11734-022-00731-2

THE EUROPEAN PHYSICAL JOURNAL SPECIAL TOPICS

Regular Article

Problem of power spectra estimation in application to the analysis of heart rate variability

Yurii M. Ishbulatov[1,2,3,a], Vladimir I. Gridnev[3,b], Vladimir I. Ponomarenko[1,2,c], Dmitry M. Ezhov[1,d], Mikhail D. Prokhorov[1,2,e], Anton R. Kiselev[4,f], and Anatoly S. Karavaev[1,2,3,g]

[1] Institute of Physics, Saratov State University, 83 Astrakhanskaya St., Saratov 410012, Russia
[2] Laboratory of Modelling in Nonlinear Dynamics, Saratov Branch of the Institute of Radio Engineering and Electronics of Russian Academy of Sciences, 38 Zelyonaya St., Saratov 410019, Russia
[3] Research Institute of Cardiology, Saratov State Medical University, 112 Bolshaya Kazachya St., Saratov 410012, Russia
[4] Coordinating Center for Fundamental Research, National Medical Research Center for Therapy and Preventive Medicine, 10 Petroverigsky Per., Moscow 101990, Russia

Received 9 October 2022 / Accepted 28 November 2022

Abstract We investigated how the parameters of the spectral analysis affect standard deviation and error of the estimation of well-known indices for the heart rate variability. We compared the nonparametric Fourier transform to the parametric approach based on autoregressive models. We also investigated how the precision of the indices estimation depends on the choice of the window function, parameterization of the Bartlett's method, and the lengths of time series. For each set of parameters, we calculated the sensitivity and specificity of the resulting indices when diagnosing arterial hypertension. To isolate and investigate the errors caused by inaccuracy of the spectral analysis itself, we conducted our study using the mathematical models of heart rate variability for healthy subjects and arterial hypertension patients, for which the correct values of the spectral indices are known. The obtained results suggest that the analysis of 20-min signals, comparing to 5-min signals, significantly decreases the standard deviation of the estimations and increases both their sensitivity and specificity. We found no advantages of using the parametric approach over the Fourier transform. We have shown that application of the Hann's window function and normalization of the spectral indices decreases the sensitivity and specificity of the medical diagnostics.

1 Introduction

Spectral analysis of the heart rate variability (HRV) is used to noninvasively estimate the depth of heart rate frequency modulation by the autonomic control of circulation. The gold standard method for measuring HRV is the extraction of RR intervals (RRI), which is a sequence of time intervals of the R peaks in the electrocardiogram (ECG) signals [1, 2]. The spectral power in the 0.04–0.15 Hz frequency band (LF index) is mainly associated with the heart rate modulation by the sympathetic part of the autonomic control, while the spectral power in the 0.15–0.4 Hz frequency band (HF index) is mainly associated with the parasympathetic part of the autonomic control [3–5].

Low values of the LF and HF indices are associated with the coronary artery disease [6] pre-clinical arterial hypertension [7], and higher 4-year mortality risk among elderly patients [8] and myocardium infarction patients [9]. Decreased RRI variability is linked to the higher risk of cardiovascular system (CVS) diseases among diabetic patients [10–12] and healthy subjects [13–16]. In [17], the spectral analysis was used as a more cost-effective substitute for the polysomnography when screening for the obstructive sleep apnea hypopnea syndrome.

In recent years, viability of the HRV spectral analysis for early screening continues to grow [18, 19] due to rapid development and popularization of variable commercial devices that can register the photoplethysmogram (PPG) signals [20]. Recent studies [21, 22] have

Vladimir I. Gridnev, Vladimir I. Ponomarenko, Dmitry M. Ezhov, Mikhail D. Prokhorov, Anton R. Kiselev, Anatoly S. Karavaev contributed equally to this work.

[a] e-mail: ishbulatov95@mail.ru (corresponding author)
[b] e-mail: gridnev@cardio-it.ru
[c] e-mail: ponomarenkovi@gmail.com
[d] e-mail: ezhovdmitryi@yandex.ru
[e] e-mail: mdprokhorov@yandex.ru
[f] e-mail: antonkis@list.ru
[g] e-mail: karavaevas@gmail.com

Published online: 04 January 2023

shown that for relaxed, healthy subjects, the difference between the RRI and PPI, the sequence of time intervals between the systolic peaks in PPG, is not statistically significant.

Despite the aforementioned facts, spectral analysis of the HRV is not prominent in the applied medicine [23]. One of the main reasons for it is high variability of the LF and HF indices due to circadian rhythms [24] and other factors [25–28] leading to a nonstationary behavior of HRV and individual characteristics of the patients. In grand-scale study [20], the authors investigated 8 million 24-h PPG signals, recorded using "Fitbit" fitness bracelets. This study has shown that the amplitude of the circadian oscillations of the LF and HF indices was 40% of the mean value. In 60-year-old males, the mean value of the LF index was 66.5% lower than in 20-year-old males. In elderly females, the LF index was 69.3% lower than in young females. According to [20], the values of the HF indices decrease in elderly males and females by 82.0% and 80.9%, respectively, due to aging. Moreover, even for individuals of the same age, the spectral indices estimated at the same time of day shows variation of about 100% in relation to the mean value.

Another cause of variance, which is rarely discussed, is inaccuracy of the spectral analysis itself. However, investigating the inaccuracy of spectral analysis using experimental signals is a complicated task, because of various noises and other factors that cause nonstationarity of the HRV and increase the standard deviation of the estimations.

Therefore, it seems appropriate to estimate the spectra of "ideal" time series, which has similar statistical characteristics to the experimental data, but are stationary, and for which the correct values of the LF and HF indices are known. In this case, the standard deviation of the spectral indices will only be affected by the lengths of the signals and inaccuracy of the spectral analysis. We conducted this study using the model of HRV for healthy subjects and arterial hypertension (AH) patients. The studied signals were stationary, the spectral profiles were qualitatively and quantitatively similar to the experimental data, and correct values for the LF and HF indices were known.

We estimated how the parameters of the spectral analysis, when it is applied to the heart rate variability data, affect the standard deviation and error of the estimation of the LF and HF indices. We compared the nonparametric Fourier transform to the parametric approach based on autoregressive models (AR) models. We also investigated how the precision of the indices estimation depends on the choice of the window function, parameterization of the Bartlett's method, and the lengths of time series.

2 Model

To test the methods, we applied them to the time series of an AR model of the HRV (1) with two sets of parameters. The first set corresponded to healthy subjects, while the second set corresponded to AH patients.

$$X_t = \sum_{i=1}^{p} a_i X_{t-i} + \sigma_\varepsilon^2 \varepsilon_t, \tag{1}$$

where $p = 300$ is the order of the model, $a_{1,\dots i}$ and $\overline{a}$ are the parameters of the AR model, ε_t is the zero-mean Gaussian white noise with standard deviation equal to 1, and σ_ε^2 is the variance of the white noise. Using the classical Yule–Walker approach [29, 30], the parameters of the model (1) can be fitted in a way that the model power spectra will be quantitatively similar to any defined power spectra. In this study, the parameters were fitted to achieve correspondence to the model power spectra of the HRV for healthy subjects and AH patients. The model power spectra were defined as (2), with two sets of parameters. The first set corresponded to healthy subjects, while the second set corresponded to AH patients:

$$\begin{aligned} |S(f)|^2 = {} & \frac{\sigma_{\mathrm{VLF}}^2}{\sqrt{2\pi c_{\mathrm{VLF}}^2}} \exp\left(-\frac{(f-f_{\mathrm{VLF}})^2}{2c_{\mathrm{VLF}}^2}\right) \\ & + \frac{\sigma_{\mathrm{LF}}^2}{\sqrt{2\pi c_{\mathrm{LF}}^2}} \exp\left(-\frac{(f-f_{\mathrm{LF}})^2}{2c_{\mathrm{LF}}^2}\right) + \cdots \\ & + \frac{\sigma_{\mathrm{HF}}^2}{\sqrt{2\pi c_{\mathrm{HF}}^2}} \exp\left(-\frac{(f-f_{\mathrm{HF}})^2}{2c_{\mathrm{HF}}^2}\right) + \frac{1}{a_{\mathrm{T}} f + b_{\mathrm{T}}}, \end{aligned} \tag{2}$$

where $f_{\mathrm{VLF}}, f_{\mathrm{LF}}$, and f_{HF} are the frequencies of the main spectral peaks, which are present in the experimental data; $c_{\mathrm{VLF}}, c_{\mathrm{LF}}$, and c_{HF} are the parameters that define the widths of the peaks, $\sigma_{\mathrm{VLF}}, \sigma_{\mathrm{LF}}$, and σ_{HF} are the parameters that define the height of the peaks, a_{T} and b_{T} are the parameters of the $1/f$ trend under the HRV peaks. Function (2) can quantitatively and qualitatively simulate the HRV spectra for healthy subjects and AH patients. We fitted the parameters independently for both cases, so that the power density in the very low frequency (VLF) (0.004–0.04 Hz), LF (0.04–0.15 Hz) and HF (0.15–0.4 Hz) frequency bands of the HRV was equal to the experimental data [31]. For a healthy subject, the experimental values were $\mathrm{VLF\_norm} = 710\ \mathrm{ms}^2$, $\mathrm{LF\_norm} = 452\ \mathrm{ms}^2$, and $\mathrm{HF\_norm} = 552\ \mathrm{ms}^2$, and for a AH patient—$\mathrm{VLF\_hyp} = 571\ \mathrm{ms}^2$, $\mathrm{LF\_hyp} = 378\ \mathrm{ms}^2$, and $\mathrm{HF\_hyp} = 419\ \mathrm{ms}^2$. Fitted parameters of the function (2) are listed in Table 1, while the functions themselves are shown in Fig. 1 alongside with power spectra, estimated from the model time series.

From the spectra, modeled using the function (2), we reconstructed the autocovariance functions, which were equal to the inverse Fourier transform of the power spectra:

$$\psi(\tau) \approx \mathrm{Re}\left(\mathrm{FT}^{-1}\left(|S(f)|^2\right)\right), \tag{3}$$

Table 1 Parameters of the functions that approximate the profiles of the real HRV power spectra for healthy subjects and AH patients

Parameters	f_{VLF}, Hz	f_{LF}, Hz	f_{HF}, Hz	c_{VLF}, Hz	c_{LF}, Hz	c_{HF}, Hz
Healthy	0.05	0.1	0.3	0.011	0.022	0.042
Hypertonic	0.05	0.1	0.3	0.011	0.022	0.042
Parameters	σ_{VLF}, ms Hz$^{0.5}$	σ_{LF}, ms Hz$^{0.5}$	σ_{HF}, ms Hz$^{0.5}$	a_{T}, Hz ms^2	b_{T}, Hz	
Healthy	0.158	0.078	0.097	$592df$	4	
Hypertonic	0.135	0.063	0.075	$592df$	4	

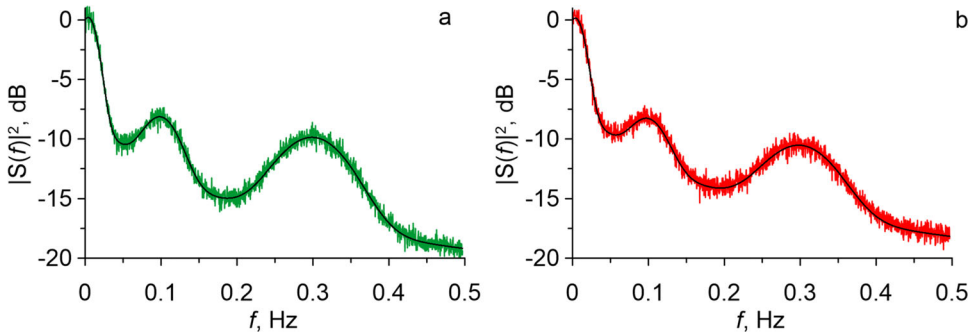

Fig. 1 Black lines show the model HRV power spectra, simulating the data from healthy subjects and AH patients. The power spectra estimated from time series of AR models are shown by green line for a healthy subject (**a**), and by red line for an AH patient (**b**)

where τ is the time delay, and FT^{-1} is the inverse Fourier transform.

For the function (2), $\psi(\tau)$ dropped to zero at $\tau \approx 75$ s, and we used the time step of 0.25 s when generating the RRI. The parameters of the AR models we estimated from the first 300 values of $\psi(\tau)$ using the Yule–Walker approach [29, 30]. This method requires the solving the system of linear equations:

$$\begin{bmatrix} \psi(0) & \psi(-1) & \psi(-2) & \dots & \dots & \psi(1-p) \\ \psi(1) & \psi(0) & \psi(-1) & \dots & \dots & \psi(2-p) \\ \dots & & & & & \\ \psi(p-1) & \dots & \dots & \psi(2) & \psi(1) & \psi(0) \end{bmatrix} \begin{bmatrix} a_1 \\ a_2 \\ \dots \\ a_n \end{bmatrix} = \begin{bmatrix} \psi(1) \\ \psi(2) \\ \dots \\ \psi(n) \end{bmatrix}. \tag{4}$$

If we to denote the quadratic Toeplitz matrix on the left side of (4) as $\overline{R}$, and the vector on the right as $\overline{r}$, then the vector of AR model parameters $\overline{a}$ can be calculated as:

$$\overline{a} = \overline{R}^{-1} \times \overline{r}. \tag{5}$$

After calculating the vector $a_{1,\dots i}$, the final missing parameter σ_ε^2 from (1) can be calculated as:

$$\sigma_\varepsilon^2 = \psi(0) - \sum_{i=1}^{p} a_i \psi(-i). \tag{6}$$

3 Methods

The algorithm for the estimation of spectral indices from the HRV follows the recommendations of the European Society of Cardiology and the North American Society of Pacing and Electrophysiology [1]. It is recommended to analyze 5-min time series, using the Fourier transform or parametric approach, based on AR modeling. The order of the AR model should be 8–20. It also advised to use a window function, such as the Hann's window function. When using the Hann's window, we matched its lengths with the lengths of the time series. Both absolute and normalized values of the LF and HF indices can be used. The normalized indices are calculated according to formulas (7) and (8):

$$\mathrm{LFn} = \frac{\mathrm{LF}}{\mathrm{LF} + \mathrm{HF}} \tag{7}$$

and

$$\mathrm{HFn} = \frac{\mathrm{HF}}{\mathrm{LF} + \mathrm{HF}}. \tag{8}$$

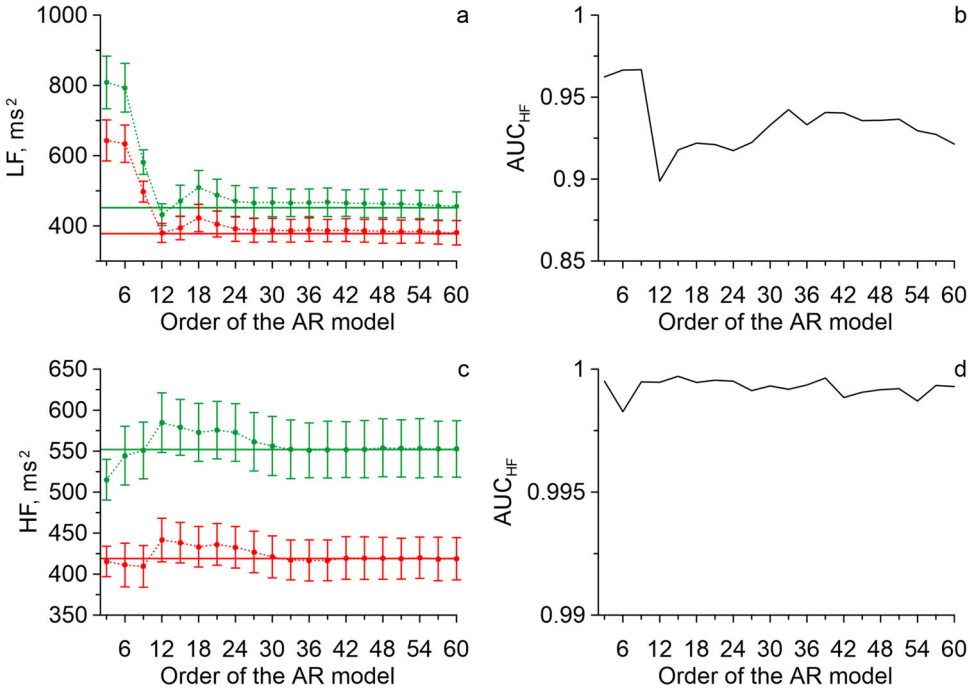

Fig. 2 Panel **a** shows the accuracy of the LF index estimations for different orders of the AR models used in a parametric method for estimation of the power spectra. The points show the mean values of the LF index for each order of the AR model, and the whiskers show the standard deviation. The indices estimated for healthy subjects are shown in green, and the indices estimated for AH patients are shown in red. We used 20-min time series. Solid lines of corresponding colors show the correct values of the LF indices. Panel **b** shows the AUC's calculated when comparing the distributions of the LF indices estimated for the model HRV of healthy subjects and AH patients for each order of the AR model. Panels **c** and **d** show similar data, but for the HF indices

Another factor we want to analyze is the application of the Bartlett's method. The method idea is to divide the time series into separate, sometimes overlapping, time windows, and to estimate the power spectra separately for different sections of time series. The final power spectrum is calculated by averaging the power spectra for different time windows. The main parameter of this approach is, therefore, the size of time windows.

In Sect. 4, we estimated the inaccuracy of the calculated spectral indices for different parameters of the spectral analysis, including the lengths of time series, method for estimation of the spectrum, and order of the AR model for the parametric approach. For each set of parameters, we estimated 1000 LF, HF, LFn and HFn indices for the model HRV both for healthy subjects and AH patients. Then, we estimated the differences between the mean values of estimated indices and experimental values from [31], standard deviations for the distributions of the estimated values, and their specificity and sensitivity when diagnosing arterial hypertension. The sensitivity was measured as a true positive rate (TPR), which is a probability of a positive test, conditioned on truly being positive. The specificity was measured as 1 − FPR, where FPR is the false positive rate, a probability of a positive test, conditioned on truly being negative. Additionally, we calculated the area under each of ROC curves (AUC).

4 Results

We compared the Fourier transform to the parametric approach based on the AR modeling. On the one hand, the parametric approach can be more accurate for short time series. On the other hand, finding a proper order of an AR model is not a trivial task. Therefore, it is important to compare the methods for each particular type of time series.

Figure 2 shows how accurately the LF and HF indices are estimated when using the AR models of different orders. We tested the orders from 3 to 60 with a step of 3 orders. AR models of different orders were used to estimate the power spectra of 1000 model HRV for healthy subjects and 1000 model HRV for AH patients. The duration of model realizations was 20 min. Therefore, we obtained the distributions of spectral indices estimations for model healthy HRV (LF_{norm} and HF_{norm}) and model AH HRV (LF_{hyp} and HF_{hyp}). We calculated the mean values and standard deviations for each distribution, and ROC curves and AUC for LF_{norm}–LF_{hyp} and HF_{norm}–HF_{hyp} pairs of distributions.

Figure 2a shows that when using the model order less than 24–30, the mean values of the estimations differ from the correct values, especially for the LF index. Therefore, our results suggest using AR models of order 30 and more. It is safe to assume that for a real data

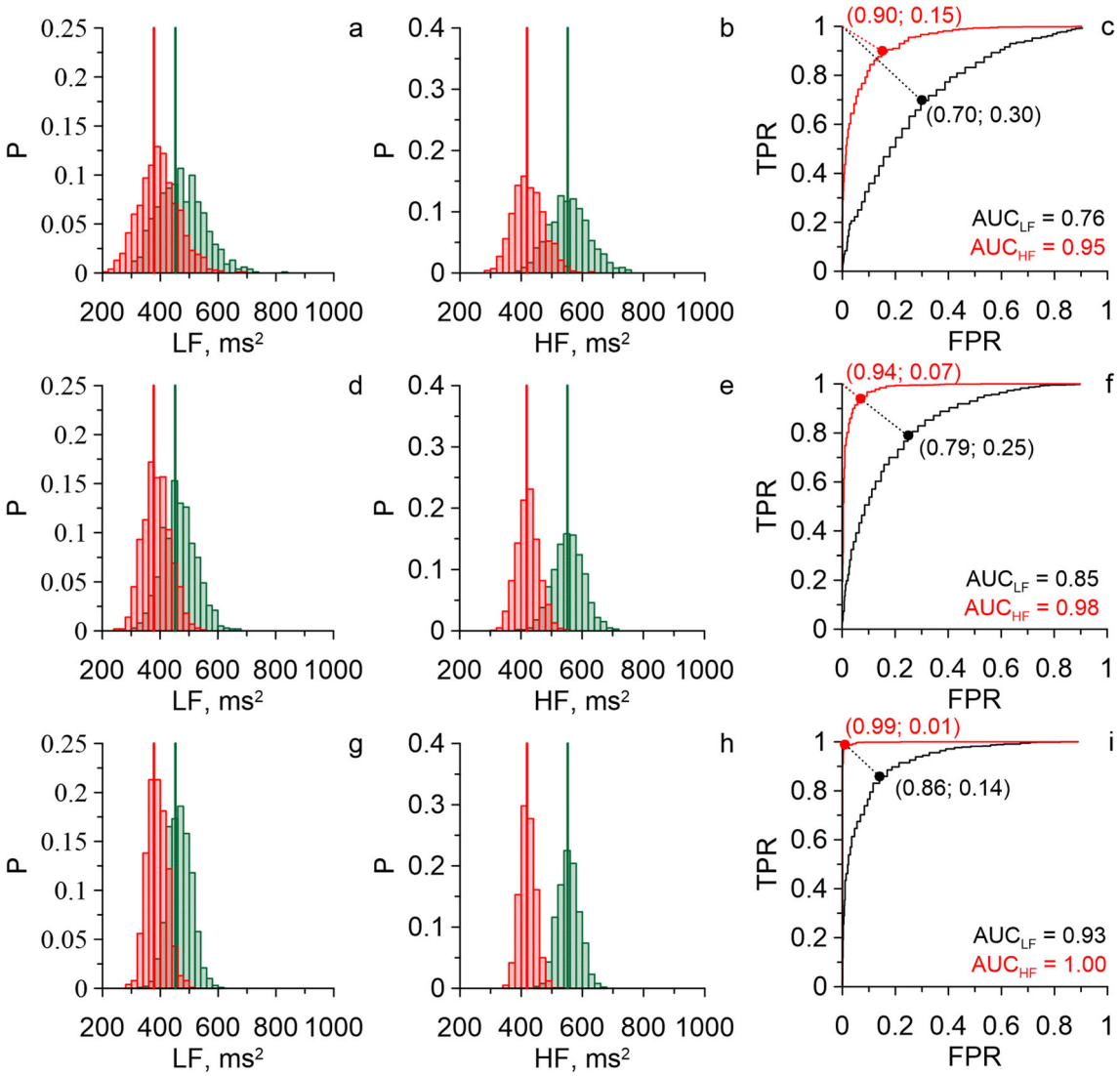

Fig. 3 Distributions of the LF and HF indices, and corresponding ROC-curves, estimated for the model time series of different lengths. We used the parametric approach based on fitting of an AR model of order 30 to estimate the power spectra. We did not apply the window functions and did not use the Bartlett's method. Panels **a**–**c** are for 5-min time series. Panels **d**–**f** are for 10-min time series. Panels **g**–**i** are for 20-min time series. Distributions for healthy subjects are shown in green and distributions for AH subjects are shown in red. Solid green and red vertical lines show the correct values of the LF and HF indices

with even more complex spectra, the adequate order of the AR model should not be lower.

We also applied to the data the automatic algorithm that chooses the order of the AR models, based on calculation of the final prediction error. When analyzing the 3-min time series, the estimated orders were 17 ± 8 and 14 ± 7 (mean $\pm$ standard deviation) for the models of healthy HRV and AH HRV, respectively. When analyzing the 10-min time series, the estimated orders were 27 ± 8 and 23 ± 9; for 20-min signals: 32 ± 3 and 31 ± 5; for 40-min signals: 34 ± 3 and 33 ± 3 for healthy HRV and AH HRV, respectively. The automatically estimated order increases with the lengths of a time series and achieve a plateau for 20-min time series at a value similar to the results we obtained from Fig. 2.

Figure 3 shows the distributions of the estimated LF and HF indices, and corresponding ROC curves, obtained for the model healthy HRV (green histograms) and model AH HRV (red histograms). We analyzed 5-min time series (panels a–c), 10-min time series (panels d–f) and 20-min time series (panels g–i) using a parametric approach based on AR modeling (the order of the model was 30). We applied no window functions in Fig. 3.

For 5-min time series, the AUC for the LF index (AUC_LF) was 0.76, while both specificity and sensitivity were approximately 70%. AUC_HF was 0.95, with specificity and sensitivity of 85%. Estimated values of the spectral indices were $\mathrm{LF}'_{\mathrm{norm}} = 472 \pm 85$; $\mathrm{LF}'_{\mathrm{hyp}} = 395 \pm 66$; $\mathrm{HF}'_{\mathrm{norm}} = 560 \pm 69$; and $\mathrm{HF}'_{\mathrm{hyp}} = 426 \pm 52$

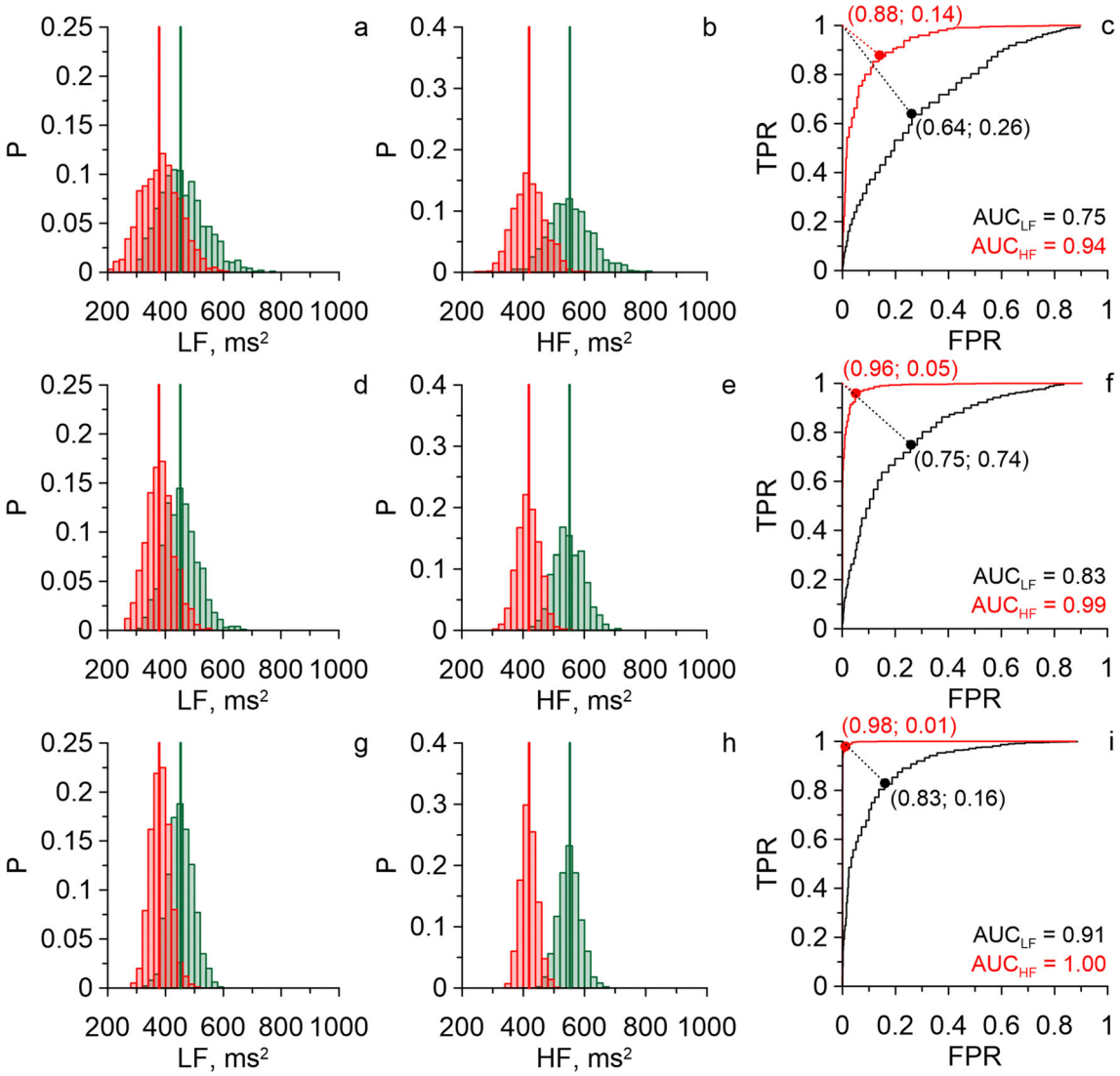

Fig. 4 Distributions of the LF and HF indices, and corresponding ROC curves, estimated for model time series of different lengths, when using the Fourier transform to estimate the power spectra. We did not apply the window functions and did not use the Bartlett's method. Panels **a**–**c** are for 5-min time series. Panels **d**–**f** are for 10-min time series. Panels **g**–**i** are for 20-min time series. Distributions for healthy subjects are shown in green and distributions for AH subjects are shown in red. Solid green and red vertical lines show the correct values of the LF and HF indices

(mean ± standard deviation), with correct values being $\mathrm{LF\_norm} = 451$; $\mathrm{LF\_hyp} = 378$; $\mathrm{HF\_norm} = 552$; and $\mathrm{F\_hyp} = 419$. For 10-min time series, the $\mathrm{AUC\_LF}$ was 0.85, with specificity and sensitivity of approximately 80%. $\mathrm{AUC\_HF}$ was 0.98, with specificity and sensitivity of approximately 95%. Estimated values of the spectral indices were $\mathrm{LF'_{norm}} = 469 \pm 58$; $\mathrm{LF'_{hyp}} = 387 \pm 49$; $\mathrm{HF'_{norm}} = 556 \pm 50$; and $\mathrm{HF'_{hyp}} = 421 \pm 35$. For 20-min time series, the $\mathrm{AUC\_LF}$ was 0.93, with specificity and sensitivity of approximately 85%. $\mathrm{AUC\_HF}$ was 1.00, with specificity and sensitivity of approximately 99%. Estimated values of the spectral indices were $\mathrm{LF'_{norm}} = 467 \pm 40$; $\mathrm{LF'_{hyp}} = 388 \pm 33$; $\mathrm{HF'_{norm}} = 553 \pm 35$; and $\mathrm{HF'_{hyp}} = 420 \pm 25$.

Therefore, Fig. 3 shows that distributions of the estimated indices LF′ and HF′ are narrower for longer time series that increases both sensitivity and specificity when using the spectral analysis to diagnose AH. Error of estimation also decreases. The increase in the accuracy is more prominent for the LF indices. We think it is due to the period of the LF oscillations being longer, which leads to a small number of full oscillations in the 5-min time series.

Figure 4 shows the distributions of the LF and HF indices, and corresponding ROC curves, estimated from 5-min model time series (panels a–c), 10-min time series (panels d–f), and 20-min time series (panels g–i). For Fig. 4, we used the Fourier transform to estimate the power spectra, without applying the window functions

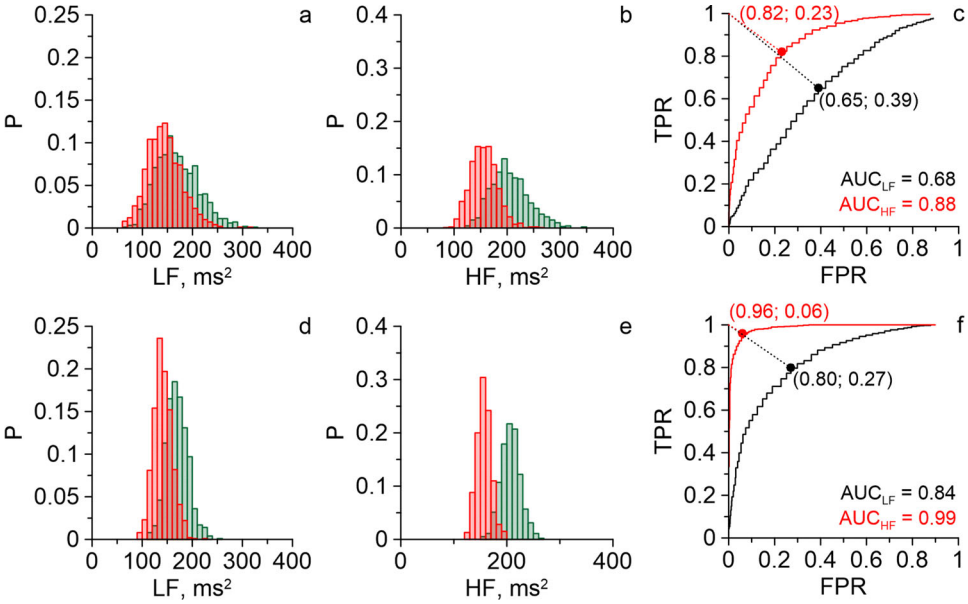

Fig. 5 Distributions of the LF and HF indices, and corresponding ROC curves, estimated for model time series of different lengths, when using the Fourier transform to estimate the power spectra. We applied the Hann's window functions and did not use the Bartlett's method. Panels **a**–**c** are for 5-min time series. Panels **d**–**f** are for 20-min time series. Distributions for healthy subjects are shown in green, and distributions for AH subjects are shown in red

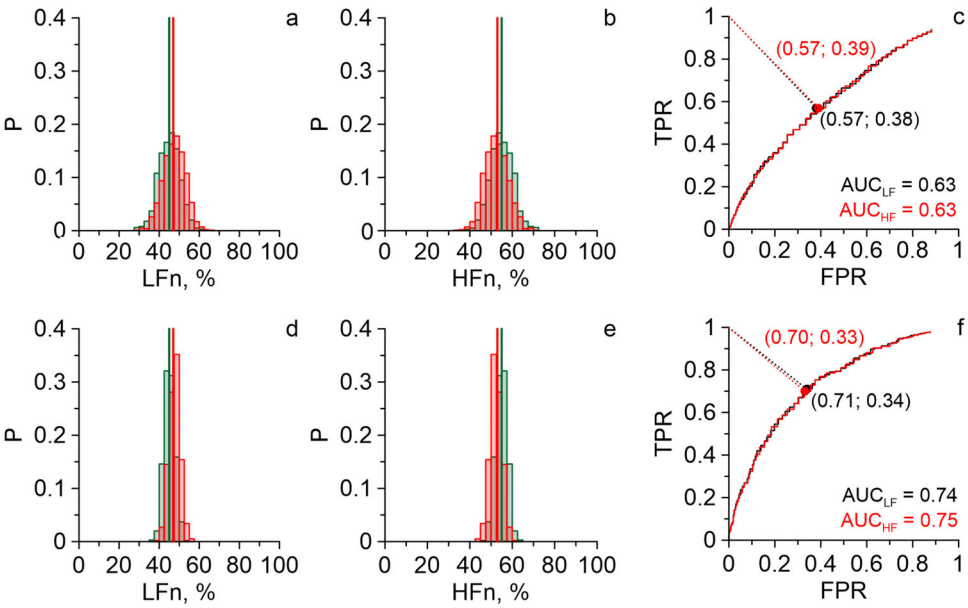

Fig. 6 Distributions of the normalized LFn and HFn indices, and corresponding ROC-curves, estimated for model time series of different lengths, when using the Fourier transform to estimate the power spectra. We did not apply the window functions and did not use the Bartlett's method. Panels **a**–**c** are for 5-min time series. Panels **d**–**f** are for 20-min time series. Distributions for healthy subjects are shown in green, and distributions for AH subjects are shown in red

and Bartlett's method. Figure 4 is conceptually similar to Fig. 3, with the only difference being the application of a nonparametric approach to estimate the spectra. The results are also quantitatively similar, and the parametric approach shows no advantages over the Fourier transform.

Figure 5 shows the distributions of the LF and HF indices, and corresponding ROC curves, estimated from 5-min model time series (panels a–c) and 20-min time series (panels d–f). For Fig. 5, we used the Fourier transform to estimate the power spectra. We did not use the Bartlett's method, but we applied the Hann's window function. Figure 5 shows that application of this window function decreases both sensitivity and specificity when diagnosing arterial hypertension: AUC_LF was 0.68 and AUC_HF was 0.88 for 5-min time series. (AUC_LF was 0.76 and AUC_HF was 0.95 for the time series of the same lengths when we did not apply the window function.) For 20-min time series, AUC_LF was 0.84 and AUC_HF was 0.99, comparing to the AUC_LF = 0.93 and AUC_HF = 1.00 for the time series of the same lengths when we did not apply the window function. Moreover, the application of the window function decreases the absolute values of the spectral indices by a factor 2.6–2.7: LF'_{norm} was 174 ± 22, LF'_{hyp} was 145 ± 18, HF'_{norm} was 208 ± 17, and HF'_{hyp} was 157 ± 13 when analyzing 20-min time series. For the same reason, the correct values of the LF and HF indices are not shown in Fig. 5.

Figure 6 shows the distributions of the normalized LFn and HFn indices, and corresponding ROC curves, estimated from 5-min model time series (panels a–c)

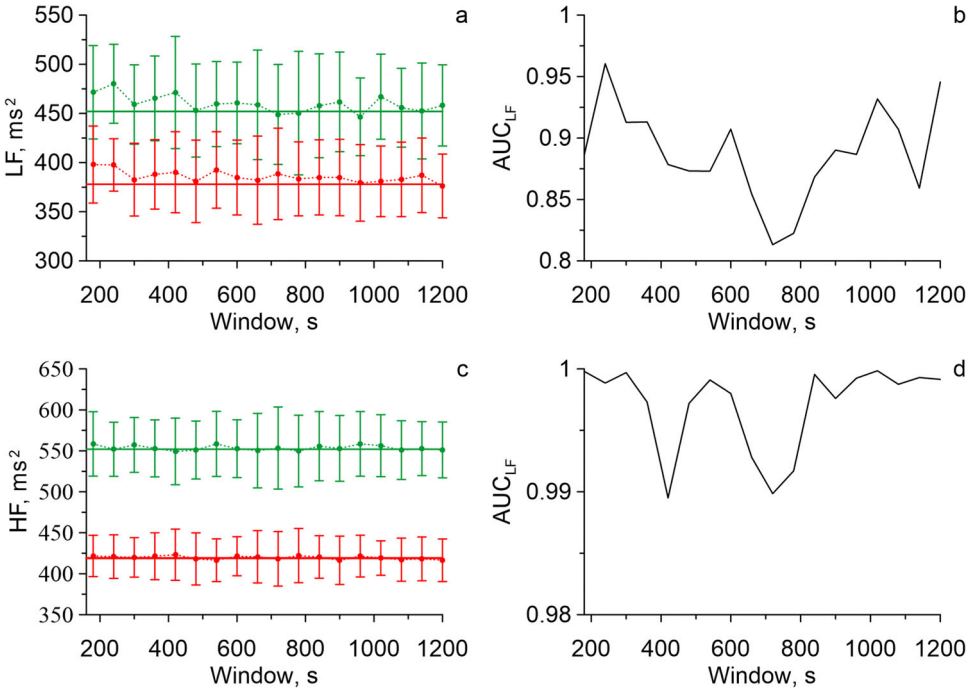

Fig. 7 Panel **a** shows the accuracy of the LF index estimations for different sizes of time windows when using the Bartlett's method to estimate the power spectra. To estimate the spectrum in each particular time window, we used a parametric method, with AR model of order 30 and did not apply the window functions. The points show the mean values of the LF index for each window size, and the whiskers show the standard deviation. The indices estimated for healthy subjects are shown in green, and the indices estimated for AH patients are shown in red. We used 20-min time series. Solid lines of corresponding colors show the correct values of the LF indices. Panel **b** shows the AUC's calculated when comparing the distributions of the LF indices estimated for the model HRV of healthy subjects and AH patients for each window size. Panels **c** and **d** show similar data, but for the HF indices

and 20-min time series (panels d–f). For Fig. 6, we used the Fourier transform to estimate the power spectra. We did not use the Bartlett's method and did not apply the Hann's window function. Figure 6 shows that the distributions of the normalized indices overlap to a much larger degree, comparing to the absolute indices, and AUC values are lower than in Fig. 4. The normalized indices show lower sensitivity and specificity because in AH patients both absolute values of the LF and HF indices are lower [31]. Because of that by normalizing the spectral indices by a factor of (LF + HF), we exclude important diagnostic information.

Figure 7 explores how the application of Bartlett's approach affects the accuracy of estimation of the LF and HF indices, namely the mean error of estimation, standard deviation of the estimated values, and corresponding AUC's. The bottom axis of the plots (a–d) shows the lengths of the time windows into which we divided the 20-min time series. For Fig. 7, we used a parametric approach based on AR modeling (the order of the model was 30) to estimate the power spectra, and we applied no window functions. Figure 7 shows that application of Bartlett's method gives no advantages in this case. When the time series is divided into very short time windows (3–5 min), the mean error of the LF index estimation increases, similarly to the case of short time series (Fig. 4). Application of the window function to each time window did not improve the sensitivity or specificity.

5 Discussion

Obtained results show that when analyzing 5-min model time series, we cannot expect sensitivity and specificity of over 70% when using spectral analysis to diagnose AH. The experimental sequences of RRI are also affected by colored noises of various origins, circadian rhythms, nonstationarity and other factors that will inevitably lower the sensitivity and specificity. Based on that, we conclude that 5-min time series is too short even for screening diagnostics. The use of 20-min time series seems more appropriate, since the sensitivity and specificity rise from 70 to 85% for the LF index, and from 90 to 99% for the HF index. We believe that longer time series is more appropriate for both the screening diagnostics and estimating the dynamics of spectral indices over 24-h period.

Figure 5 shows that application of the Hann's window function decreases sensitivity and specificity of the spectral indices, and, therefore, should be used with caution. Moreover, the application of window functions

decreases the overall power of a signal by a factor that depends on the shapes of both a particular signal and the window function. Therefore, we assume it is necessary to indicate the window function; otherwise, the results of the spectral analysis cannot be properly interpreted and compared to other data.

Figure 6 shows that in our model study, the normalized indices LFn and HFn have lower sensitivity and specificity than absolute values of LF and HF. As was mentioned in the "Results" section, we assume that normalized indices show lower sensitivity and specificity because in AH patients, both absolute values of LF and HF indices are lower [31], and by normalizing the spectral indices by a factor of (LF + HF), we exclude important diagnostic information. The obtained results show that normalized and absolute indices contain different diagnostic information, have different range of application, and, in our opinion, should be used together.

We also would like to list the limitations of our model and our study. The model intentionally did not take into account nonstationarity of the real HRV [24], impact of movement artifacts, measurement noises, and circadian rhythms because we wanted to isolate and study the errors caused by the inaccuracy of the spectral analysis itself. Due to that decision, the model cannot give reliable estimations of the sensitivity and specificity that are expected when analyzing real data [24–28], especially the data of long-term monitoring. Investigation of this problem requires modification of the model.

6 Conclusion

Our study has shown that when applying the spectral analysis to 5-min heart rate variability data to diagnose arterial hypertension, both sensitivity and specificity of diagnostics is limited to 70% for the LF index and 90% for the HF index, and is, likely, significantly lower when analyzing real noisy and nonstationary data. The analysis of 20-min data increases the sensitivity to 85% for the LF index and 99% for the HF index. In our opinion, the analysis of 20-min time series is preferable for both screening and estimation of the dynamics of spectral indices over 24-h period.

It was also shown that parametric approach to estimation of the power spectra, based on AR modeling, has no advantages over the Fourier transform for this particular type of data. When using AR models of order 30 and higher, the results are quantitatively similar, but when using AR models of lesser orders, the spectral indices are estimated with significant errors.

Application of the Bartlett's method had no effect on the sensitivity and specificity of the diagnostics. Application of the Hann's window function decreases both sensitivity and specificity, regardless of other parameters of the spectral analysis.

The normalized spectral indices LFn and HFn had much lower sensitivity and specificity than the absolute indices LF and HF, because for the arterial hypertension patients, the total power LF + HF contains important diagnostic information, and normalization loses it. The obtained results show that normalized and absolute indices contain different diagnostic information, have different range of application, and, in our opinion, should be used together.

Funding This work was supported by the Project of RF Government, Grant no. 075-15-2022-1094.

Data availability The datasets generated and/or analyzed during the current study are available from the corresponding author on reasonable request.

Declarations

Conflict of interest The authors have no relevant financial or non-financial interests to disclose.

References

1. Task Force of the European Society of Cardiology and the North American Society of Pacing and Electrophysiology. Circulation (1996). https://doi.org/10.1161/01.CIR.93.5.1043
2. M.D. Prokhorov, A.S. Karavaev, Yu.M. Ishbulatov, V.I. Ponomarenko, A.R. Kiselev, J. Kurths, Phys. Rev. E (2021). https://doi.org/10.1103/PhysRevE.103.042404
3. D.L. Eckberg, Circulation (1997). https://doi.org/10.1161/01.CIR.96.9.3224
4. D.S. Goldstein, O. Bentho, M.Y. Park, Y. Sharabi, Exp. Physiol. (2011). https://doi.org/10.1113/expphysiol.2010.056259
5. G.A. Reyes del Paso, W. Langewitz, L.J. Mulder, A. van Roon, S. Duschek, Psychophysiology (2013). https://doi.org/10.1111/psyp.12027
6. M.J. Niemelä, K.E. Airaksinen, H.V. Huikuri, J. Am. Coll. Cardiol. (1994). https://doi.org/10.1016/0735-1097(94)90379-4
7. J.P. Singh, M.G. Larson, H. Tsuji, J.C. Evans, C.J. O'Donnell, D. Levy, Hypertension (1998). https://doi.org/10.1161/01.HYP.32.2.293
8. H. Tsuji, F.J. Venditti Jr., E.S. Manders, J.C. Evans, M.G. Larson, C.L. Feldman, D. Levy, Circulation (1994). https://doi.org/10.1161/01.CIR.90.2.878
9. A.J. Camm, C.M. Pratt, P.J. Schwartz, H.R. Al-Khalidi, M.J. Spyt, M.J. Holroyde, R. Karam, E.H. Sonnenblick, J.M. Brum, Circulation (2004). https://doi.org/10.1161/01.CIR.0000117090.01718.2A
10. D. Liao, C. Mercedes, G.W. Evans, W.E. Cascio, G. Heiss, Diabetes (2002). https://doi.org/10.2337/diabetes.51.12.3524
11. R.M. Carney, J.A. Blumenthal, K.E. Freedland, P.K. Stein, W.B. Howells, L.F. Berkman, L.L. Watkins, S.M. Czajkowski, J. Hayano, P.P. Domitrovich, A.S. Jaffe, Arch. Intern. Med. (2005). https://doi.org/10.1001/archinte.165.13.1486
12. M.T. La Rovere, G.D. Pinna, S.H. Hohnloser, F.I. Marcus, A. Mortara, R. Nohara, J.T. Bigger Jr., A.J. Camm, P.J. Schwartz, Circulation (2001). https://doi.org/10.1161/01.CIR.103.16.2072

13. S. Hillebrand, K.B. Gast, R. de Mutsert, C.A. Swenne, J.W. Jukema, S. Middeldorp, F.R. Rosendaal, O.M. Dekkers, EP Europace (2013). https://doi.org/10.1093/europace/eus341
14. J.M. Dekker, R.S. Crow, A.R. Folsom, P.J. Hannan, D. Liao, C.A. Swenne, E.G. Schouten, Circulation (2000). https://doi.org/10.1161/01.CIR.102.11.1239
15. V.N. Patel, B.R. Pierce, R.K. Bodapati, D.L. Brown, D.G. Ives, P.K. Stein, JACC Heart Fail. (2017). https://doi.org/10.1016/j.jchf.2016.12.015
16. P.K. Stein, J.I. Barzilay, P.H. Chaves, S.Q. Mistretta, P.P. Domitrovich, J.S. Gottdiener, M.W. Rich, R.E. Kleiger, J. Cardiovasc. Electrophysiol. (2008). https://doi.org/10.1111/j.1540-8167.2008.01232.x
17. X. Gong, L. Huang, X. Liu, C. Li, X. Mao, W. Liu, X. Huang, H. Chu, Y. Wang, W. Wu, J. Lu, PLoS One (2016). https://doi.org/10.1371/journal.pone.0156628
18. A.R. Kiselev, E.I. Borovkova, V.A. Shvartz, V.V. Skazkina, A.S. Karavaev, M.D. Prokhorov, A.Y. Ispiryan, S.A. Mironov, O.L. Bockeria, Sci. Rep. (2020). https://doi.org/10.1038/s41598-020-58196-z
19. A.R. Kiselev, A.S. Karavaev, Blood Press. (2020). https://doi.org/10.1080/08037051.2019.1645586
20. A. Natarajan, A. Pantelopoulos, H. Emir-Farinas, P. Natarajan, Lancet (2020). https://doi.org/10.1016/S2589-7500(20)30246-6
21. A. Schäfer, J. Vagedes, Int. J. Cardiol. (2013). https://doi.org/10.1016/j.ijcard.2012.03.119
22. A.S. Karavaev, A.S. Borovik, E.I. Borovkova, E.A. Orlova, M.A. Simonyan, V.I. Ponomarenko, V.V. Skazkina, V.I. Gridnev, B.P. Bezruchko, M.D. Prokhorov, A.R. Kiselev, Biophys. J. (2021). https://doi.org/10.1016/j.bpj.2021.05.020
23. R. Sassi, S. Cerutti, F. Lombardi, M. Malik, H.V. Huikuri, C.K. Peng, G. Schmidt, Y. Yamamoto, Europace (2015). https://doi.org/10.1093/europace/euv015
24. G. Vandewalle, B. Middleton, S.M. Rajaratnam, B.M. Stone, B. Thorleifsdottir, J. Arendt, D.J. Dijk, J. Sleep Res. (2007). https://doi.org/10.1111/j.1365-2869.2007.00581.x
25. M. Reardon, M. Malik, Pacing Clin. Electrophysiol. (1996). https://doi.org/10.1111/j.1540-8159.1996.tb03241.x
26. U. Zulfiqar, D.A. Jurivich, W. Gao, D.H. Singer, Am. J. Cardiol. (2010). https://doi.org/10.1016/j.amjcard.2009.12.022
27. B.Q. Farah, A. Andrade-Lima, A.H. Germano-Soares, D.G.D. Christofaro, M.V.G. de Barros, W.L. do Prado, R.M. Ritti-Dias, Pediatr. Cardiol. (2018). https://doi.org/10.1007/s00246-017-1775-6
28. K. Howorka, J. Pumprla, P. Haber, J. Koller-Strametz, J. Mondrzyk, A. Schabmann, Cardiovasc. Res. (1997). https://doi.org/10.1016/s0008-6363(97)00040-0
29. G.U. Yule, Philos. Trans. R. Soc. Lond. Ser. A 226 (1927). https://doi.org/10.1098/rsta.1927.0007
30. G. Walker, Proc. R. Soc. Lond. Ser. A 131 (1931). https://doi.org/10.1098/rspa.1931.0069
31. R.H. Fagard, K. Stolarz, T. Kuznetsova, J. Seidlerov, V. Tikhonoff, T. Grodzicki, Y. Nikitin, J. Filipovsky, J. Peleska, E. Casiglia, L. Thijs, J.A. Staessen, K. Kawecka-Jaszcz, J. Hypertens. (2007). https://doi.org/10.1097/HJH.0b013e3282efc1fe